Materials Chemistry and Physics 138 (2013) 862–869

Contents lists available at SciVerse ScienceDirect

Materials Chemistry and Physics

journal homepage: www.elsevier.com/locate/matchemphys

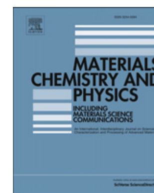

Enhancement of ferroelectric and piezoelectric properties in PZT thin films with heterolayered structure

Minh D. Nguyen [a,b,*], Chi T.Q. Nguyen [a], Thong Q. Trinh [a,c], Tai Nguyen [a], Thao N. Pham [a], Guus Rijnders [b], Hung N. Vu [a,*]

[a] International Training Institute for Materials Science (ITIMS), Hanoi University of Science and Technology, No. 1 Dai Co Viet road, Hanoi, Viet Nam
[b] Inorganic Materials Science (IMS), MESA+ Institute for Nanotechnology, University of Twente, P.O. Box 217, 7500AE Enschede, The Netherlands
[c] Institute of Engineering Physics, Hanoi University of Science and Technology, No. 1 Dai Co Viet road, Hanoi, Viet Nam

HIGHLIGHTS

► We examine the alternating heterolayered PZT thin films.
► These structures improve the ferroelectric and piezoelectric properties.
► Field-induced coupling effect induces domain switching.
► Film/film interface enhances the dielectric constant.
► Reduction in interfacial and clamping effects with increasing film thickness.

ARTICLE INFO

Article history:
Received 3 September 2012
Received in revised form
5 December 2012
Accepted 23 December 2012

Keywords:
Multilayers
Interfaces
Ferroelasticity
Ferroelectricity

ABSTRACT

This paper reports the latest experimental results of multilayered, heterolayered, and alternating heterolayered PZT thin films obtained by spin coating on $Pt/Ti/SiO_2/Si$ wafers using Zr-rich (P60) and Ti-rich (P40) solutions which were prepared by sol–gel route process. The ferroelectric and piezoelectric properties of the heterolayered and alternating heterolayered P60/P40 thin films were significantly improved when compared to those of multilayered thin films using just P60 or P40 for the same film thickness. The improved properties resulted from the field-induced coupling effect between the rhombohedral (Zr-rich) and tetragonal (Ti-rich) layers which induces domain switching. Namely, the values of the remnant polarization, dielectric constant and piezoelectric coefficient were 18.6 $\mu C\ cm^{-2}$, 1040 and 70 pm V^{-1} respectively, for alternating heterolayered P60/P40 thin films, while the properties for the purely multilayered P60 and P40 thin films were 14.6 $\mu C\ cm^{-2}$, 860 and 52 pm V^{-1}, and 17.1 $\mu C\ cm^{-2}$, 800 and 50 pm V^{-1}, respectively. The enhancement of the ferroelectric and piezoelectric properties of PZT thin films with increasing film thickness in this case could be explained by the existence of an interfacial layer and substrate clamping.

© 2013 Elsevier B.V. All rights reserved.

1. Introduction

Ferroelectric and piezoelectric thin films have received a great deal of attention in recent years for their potential applications in dynamic random access memories (DRAMs), nonvolatile ferroelectric random access memories as well as microelectromechanical systems (MEMS) [1,2]. Sensing and actuation capabilities in most of the MEMS devices utilize the piezoelectric effect, such as in bio-sensors [3–5], micro-machined ultrasonic transducers (MUTs) [6,7], accelerometers [8], and micro-pumps [9,10]. Among various piezoelectric thin-film materials; such as the well known $BaTiO_3$, AlN and ZnO; $Pb(Zr,Ti)O_3$ (PZT) thin films can offer an attractive option in microsensor and microactuator applications due to their superior ferroelectric and piezoelectric properties [11].

In bulk PZT ceramics, the maximum ferroelectric and piezoelectric properties are observed near the morphotropic phase boundary (MPB, Zr/Ti = 52/48). It results from the increased poling efficiency due to the metastable coexistence of ferroelectric tetragonal and rhombohedral phases at room temperature. The

* Corresponding authors. International Training Institute for Materials Science (ITIMS), Hanoi University of Science and Technology, No. 1 Dai Co Viet road, Hanoi, Viet Nam. Tel.: +84 438680787; fax: +84 438692963.
E-mail addresses: minh.nguyen@itims.edu.vn (M.D. Nguyen), hungvungoc@itims.edu.vn (H.N. Vu).

0254-0584/$ – see front matter © 2013 Elsevier B.V. All rights reserved.
http://dx.doi.org/10.1016/j.matchemphys.2012.12.074

poling under the applied electric field of the PZT ceramic is also easy at this composition because the spontaneous polarization within each grain can be switched to one of the 14 possible orientations (eight [111] directions and six [100] directions for rhombohedral and tetragonal phases, respectively). PZT thin films are more complex since the film properties are affected by several factors such as crystal orientation, Zr/Ti ratio, and substrate clamping. Kim et al. [12] have observed that larger polarization was obtained with increasing Ti content in the PZT thin films; whereas, higher dielectric constant and piezoelectric coefficient were observed in the rhombohedral phase region (on the Zr-rich side) as compared to the tetragonal phase region (on the Ti-rich side). The trend in the dielectric constant and piezoelectric coefficient d_{33} is similar to that of the bulk ceramic with the highest dielectric constant and piezoelectric coefficient at the MPB [13]. Based on the ability to fabricate PZT thin films with crystalline structures from rhombohedral to tetragonal phase by tuning the Zr/Ti ratio, the ferroelectric and piezoelectric properties undergo severe changes as well.

Heterolayered PZT thin films have recently attracted attention because of their improved ferroelectric and dielectric constants as compared to the single/multilayered thin films [14,15]. For instance, Kartawidjaja et al. [16] showed the higher values of polarization (47.7 μC cm^{-2} at maximum driving field of 1000 kV cm^{-1}) and dielectric constant (1002 at 100 Hz) for heterolayered $Pb(Zr_{30}Ti_{70})O_3$/$Pb(Zr_{70}Ti_{30})O_3$ thin films on Pt/Ti/SiO_2/Si than those of the multilayered $Pb(Zr_{70}Ti_{30})O_3$ (34.8 μC cm^{-2} and 560.9) and $Pb(Zr_{30}Ti_{70})O_3$ (37.3 μC cm^{-2} and 539.3) thin films. The enhancement in polarization for the heterolayered PZT thin film can be explained by the field induced stress and coupling effects between the layers of different structures [16,17]. This paper presents the investigations of the multilayered $[Pb(Zr_{0.6}Ti_{0.4})O_3]_{m+n}$ and $[Pb(Zr_{0.4}Ti_{0.6})O_3]_{m+n}$, heterolayered $[Pb(Zr_{0.6}Ti_{0.4})O_3]_m/[Pb(Zr_{0.4}Ti_{0.6})O_3]_n$ (m and n are the number coating layers with $m + n = 6$) and alternating heterolayered $[Pb(Zr_{0.6}Ti_{0.4})O_3/Pb(Zr_{0.4}Ti_{0.6})O_3]_N$ (N is the number of couple-coating layers, $N = 2$, 3, and 4) thin films prepared by sol–gel technique. Their ferroelectric–dielectric–piezoelectric properties are systematically investigated, in order to understand the mechanism of domain switching and residual stress in the heterolayered thin film structures. As the film thickness can strongly affect the ferroelectric and piezoelectric properties, moreover, these parameters are also investigated for the alternating heterolayered PZT thin films with different number of coating layers.

2. Experimental procedure

2.1. Sol–gel PZT thin film fabrication

The multilayered $Pb(Zr_{0.6}Ti_{0.4})O_3$ (P60) and $Pb(Zr_{0.4}Ti_{0.6})O_3$ (P40), and heterolayered $Pb(Zr_{0.6}Ti_{0.4})O_3/Pb(Zr_{0.4}Ti_{0.6})O_3$ (P60/P40) thin films were formed on Pt/Ti/SiO_2/Si wafers using solutions prepared by a sol–gel technique. Here, the PZT precursor solution was prepared from lead acetate ($Pb[OAc]_2 \cdot 3H_2O$), titanium *iso*-propoxide ($Ti[i\text{-}OPr]_4$) and zirconium *n*-propoxide ($Zr[n\text{-}OPr]_4$) in 2-methoxyethanol solvent. Each layer of the PZT films was formed by spin coating 0.4 M PZT precursor with 10 mol% excess lead content on the previously mentioned wafers at 4000 rpm for 30 s, followed by pyrolysis at 400 °C for 10 min. The process was repeated until the PZT thin films with the required coating layers were obtained. Finally, thermal annealing at 650 °C for 60 min was carried out to obtain the ferroelectric phase in the PZT thin films. The thickness of each coating layer was about 60 nm. The structures of the multilayered, heterolayered and alternating heterolayered PZT thin films in this study are shown in Fig. 1.

2.2. Cross-sectional morphology and element depth profile

The microstructure of the sol–gel PZT thin films was investigated using high-resolution scanning electron microscope (HRSEM: Zeiss-1550), as shown in Fig. 2. It can be seen that all films are considerably dense and crack-free with a thickness of 360 nm. Although, there is a little bit of difference for P60 and P40 layers when alternatively deposited to make the heterolayered films (see Fig. 2(c) and (d)) no apparent segregation can be seen in these structures.

The compositional depth profile of the thin films, interfacial layer and substrate was investigated by X-ray photoelectron spectroscopy (XPS: PHI QuanteraSXM). The XPS depth profile of the multilayered P60 and P40 thin films as well as the alternating heterolayered P60/P40 thin films having 4 layers is shown in Fig. 3. It is clear that the compositional distributions are almost constant in the thickness direction for multilayered films (Fig. 3(a) and (b)), except for the outmost surface layer and transient layer close to the surface of Pt electrodes. There exists a non-uniform profile for Zr and Ti elements of the alternating heterolayered films (Fig. 3(c)) due to the difference of their composition ratio in each PZT layer, with higher Ti intensity corresponding to P40 layers and higher Zr intensity corresponding to P60 layers. The existence of slightly

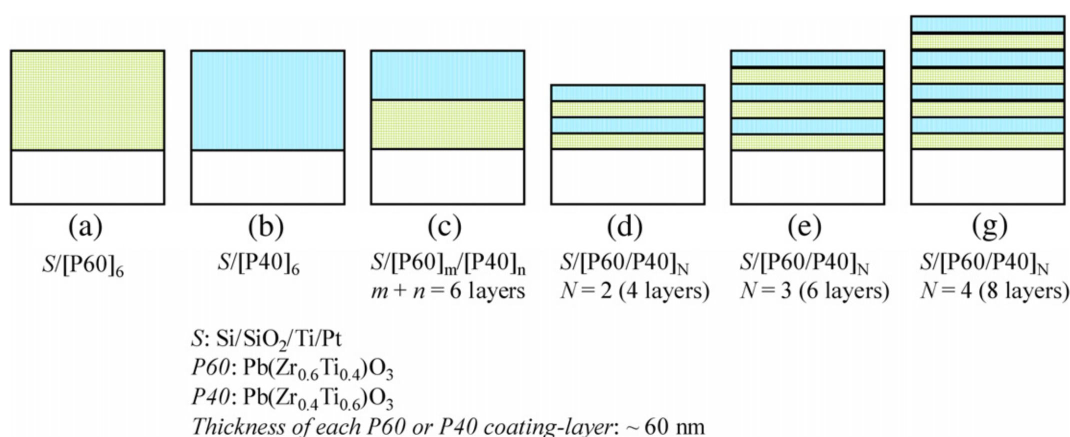

Fig. 1. Schematic diagrams of (a) multilayered thin films of $Pb(Zr_{0.6}Ti_{0.4})O_3$ with 6-coating layers ($[P60]_6$), (b) multilayered thin films of $Pb(Zr_{0.4}Ti_{0.6})O_3$ with 6-coating layers ($[P40]_6$) and (c) heterolayered thin films of $[P60]_m/[P40]_n$ ($m + n = 6$ layers); (d)–(g) alternating heterolayered thin films of $[P60/P40]_N$ with the couple-coating layer $N = 2$ (4-layers), $N = 3$ (6-layers) and $N = 4$ (8-layers). All films are coated on Pt/Ti/SiO_2/Si wafers.

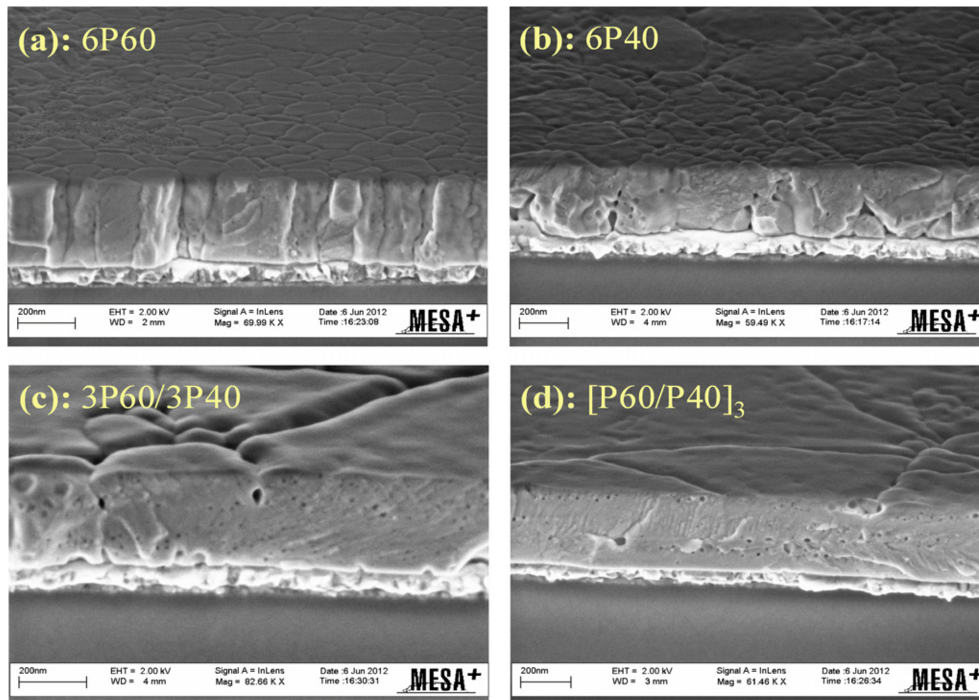

Fig. 2. Cross-sectional SEM micrographs of (a) multilayered $[P60]_6$ thin film and (b) multilayered $[P40]_6$ thin film; (c) heterolayered $[P60]_3/[P40]_3$ thin film and (d) alternating heterolayered $[P60/P40]_3$ thin film.

more lead on the surface may be due to an evaporation of the PbO during the annealing process.

2.3. Crystalline structure

The crystalline structures of the PZT thin films were analyzed by high-resolution X-ray diffraction (XRD: Bruker D8 Discover) with a Cu-Kα cathode in Bragg–Brentano geometry. The film texture and phases present in the multilayered and heterolayered PZT thin films can be seen clearly in Fig. 4(a). This result shows that all films have been crystallized at 650 °C in a perovskite structure with (100) preferred orientation and no pyrochlore phase. There is also a coexistence of P60 and P40 in the XRD traces, where P60 exhibits a rhombohedral structure while P40 exhibits a tetragonal structure (Fig. 4(b)).

2.4. Ferroelectric and piezoelectric measurements

For the electrical measurements, the Pt top-electrodes (200×200 μm^2 in size) were sputter deposited and patterned by a lift-off technique. The bottom electrode was exposed by wet-chemical etching of the PZT using a solution of *HF*, HNO_3, and *HCl*.

The polarization hysteresis (*P*–*E*) loop measurements were performed using the ferroelectric mode of the aixACCT TF-2000 analyzer. In this study, the *P*–*E* loops were performed at the applied *ac*-electric field of ±420 kV cm^{-1} and 1 kHz frequency and at room temperature. A Süss MicroTech PM300 manual probe-station equipped with a Keithley 4200 Semiconductor characterization system was used for the capacitance measurement. The capacitance–electric field (*C*–*E*) curves were measured at the applied *dc*-electric field of ±300 kV cm^{-1} with an *ac*-electric field of

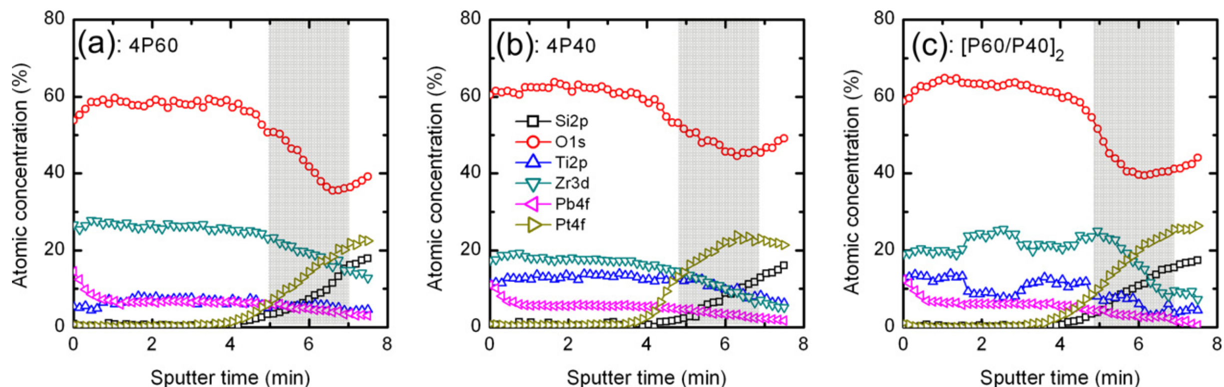

Fig. 3. XPS depth profile along the interface between the Pt bottom electrode and PZT thin film of (a) multilayered $[P60]_4$ thin film, (b) multilayered $[P40]_4$ thin film, and (c) heterolayered $[P60/P40]_2$ thin film.

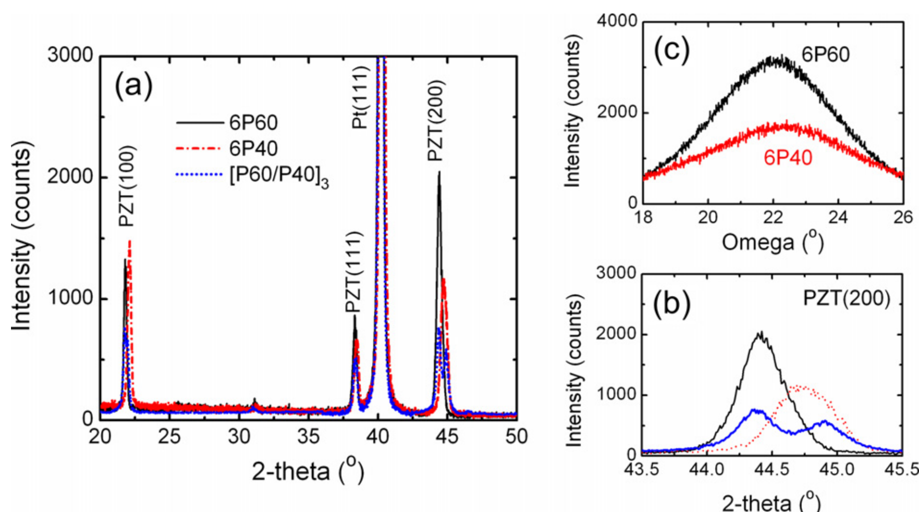

Fig. 4. (a) XRD patterns of multilayered $[P60]_6$ and $[P40]_6$ and alternating heterolayered $[P60/P40]_3$ thin films, and (b) zoom in of the PZT(200) peaks; (c) rocking curve (ω-scan) of multilayered $[P60]_6$ and $[P40]_6$ thin films at the (200)-diffraction peaks with the full-width at half maximum intensity (FWHM) of 4.6° and 5.1°, respectively.

4 kV cm^{-1} and 1 kHz frequency. The corresponding dielectric constants were calculated from these C–E curves.

The effective piezoelectric coefficient ($d_{33,f}$) of the piezoelectric thin-film capacitors was measured using a Polytech MSA-400 scanning laser Doppler vibrometer (LDV) method with a precision below 1 pm. In this study, the piezoelectric capacitor was excited by applying a sinusoidal *ac*-voltage of 3 V (or 6 V_{p-p} peak-to-peak) and at 8 kHz frequency.

3. Results and discussion

The experimental results of remnant polarization P_r and effective piezoelectric coefficient $d_{33,f}$ of the 360-nm-thick multilayered $[P60]_6$ and $[P40]_6$, heterolayered $[P60]_m/[P40]_n$ ($m + n = 6$) and alternating heterolayered $[P60/P40]_N$ ($N = 3$) thin films are shown in Figs. 5 and 6. It can be seen that the heterolayered thin films (e.g., $[P60]_3/[P40]_3$) exhibited better values of P_r and $d_{33,f}$ (17.8 μC cm^{-2} and 62 pm V^{-1}) than those of the multilayered ones, that is, 14.6 μC cm^{-2} and 52 pm V^{-1} for $[P60]_6$ films, and 17.1 μC cm^{-2} and 50 pm V^{-1} for $[P40]_6$ films.

As mentioned previously, studies have shown that the residual stress induced in the PZT thin film is known to affect the reorientation of the ferroelectric domains [18–20]. Tensile stress tends to cause domains parallel to the film surface, which leads to a reduction in polarization/piezoelectric coefficient. In contrary, compressive stress causes the domains to orient along the longitudinal direction, which in turn will cause an increase in the polarization/piezoelectric coefficient. The PZT films grown on Si substrates under biaxial tensile stress while cooling (from the annealing/firing temperature) through the Curie temperature tend to relieve such stress through the development of the a-domain orientation ($c/a < 1$), because the coefficient of thermal expansion for the Si (4.4×10^{-6} K^{-1}) substrate is smaller than that for the PZT film (6.0×10^{-6} K^{-1}) [21–23]. Finally, when the sol–gel PZT thin film is cooled down to the room temperature, the residual tensile stress is approximately in the range of 150–180 MPa for the film thickness in the range of 190–500 nm [24]. In this study, due to the cooperative interaction between two ferroelectric phases (rhombohedral 'P60' phase and tetragonal 'P40' phase), the residual stress caused by film/substrate can be decreased by the discontinuity of stress between the layers with different compositions, due to the large in-plain strain induced in the rhombohedral layers giving rise to a compressive stress on the adjacent tetragonal layers [25]. The decrease of residual tensile stress in the heterolayered film leads to the enhancement in P_r and d_{33} values [26]. For instance, the P_r and d_{33} values of alternating heterolayered $[P60/P40]_3$ and heterolayered $[P60]_3/[P40]_3$ thin films are 18.6 μC cm^{-2} and 70 pm V^{-1}, and

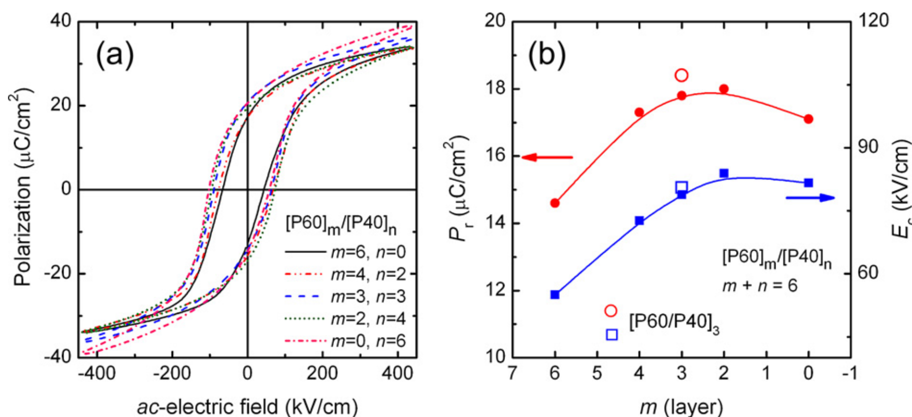

Fig. 5. (a) Polarization hysteresis loops, and (b) remnant polarization (P_r) and coercive field (E_c), of multilayered $[P60]_6$ and $[P40]_6$, and heterolayered $[P60]_3/[P40]_3$ thin films. The lines are drawn to guide the eye.

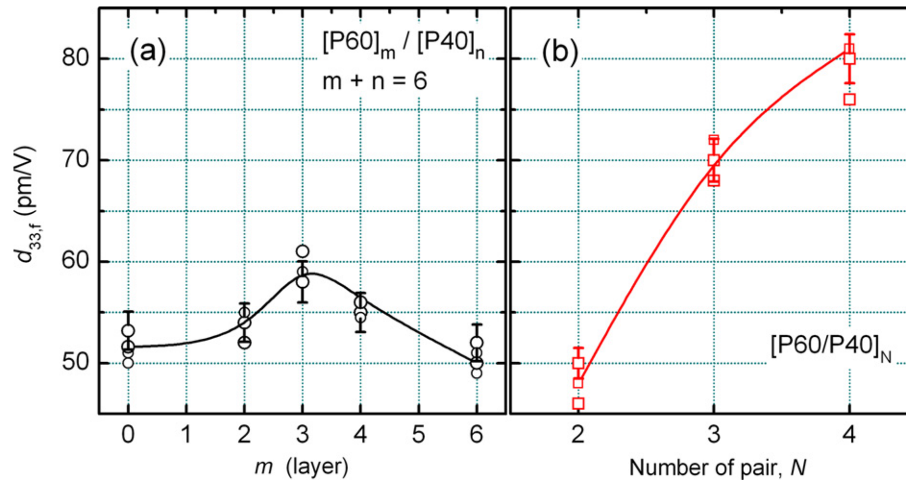

Fig. 6. Effective piezoelectric coefficient ($d_{33,f}$) of: (a) multilayered $[P60]_6$ and $[P40]_6$, and heterolayered $[P60]_3/[P40]_3$ thin films, and (b) alternating heterolayered $[P60/P40]_3$ thin films. The lines are drawn to guide the eye.

17.8 μC cm^{-2} and 62 pm V^{-1} (see Figs. 5(b) and 6), respectively. Moreover, the enhancement in ferroelectric and piezoelectric properties of the heterolayered thin films can be also explained by the field-induced coupling effect between the rhombohedral and tetragonal phase layers that induces domain switching. These enhancement factors are also used to explain the improvement of ferroelectric and piezoelectric properties in alternating heterolayered PZT thin films. The field-induced coupling effect is also called the electric field-induced rhombohedral–tetragonal phase transition, in which a remnant tetragonal phase could be preserved after removal of the electric field [25,27]. A paper published by Zhou et al. described the contribution of the field-induced coupling on the enhancement of polarization [25]. When an electric field is applied to the surface of the heterolayered film, the electric field-induced rhombohedral–tetragonal phase transition occurs in the rhombohedral layers. The polarization of the induced tetragonal phase in the rhombohedral phase is along the *c*-axis, which is normal to surface of film; on the other hand, the polarization is aligned to the electric field direction.

As can be seen in Fig. 5(b), the larger P_r values are obtained for the heterolayered films having a greater number of tetragonal layers (P40). Basically, the polarization vectors in the tetragonal phase lie along the pseudocubic {100}-direction, compared to the {111}-direction in the rhombohedral phase of the pseudocubic crystalline structure. Experimentally, the polarization measurement is along the {001}-direction and this might be the reason for the above result. In contrast, a higher dielectric constant is observed in the heterolayered films having more rhombohedral layers (P60), as shown in Fig. 7(b), because the spontaneous polarization within each grain in rhombohedral phase can be switched to one of the 8 possible orientations (eight [111] directions for the rhombohedral phase) compared to the 6 possible domain states from the tetragonal phase (six [100] directions for the tetragonal phase) and the domains in rhombohedral phase are easier to switch than the tetragonal phase.

The enhancement of dielectric constant in the heterolayered PZT thin films, as shown in Fig. 7, has been studied with capacitors in series with the contribution of the film–electrode interface. According to the widely accepted model for metal-ferroelectric-metal (*M*–*F*–*M*) structure the theoretical capacitance *C* of the single/multilayered PZT (e.g., $[P60]_6$) thin films can be expressed as follows [28–30]:

$$\frac{1}{C} = \frac{d_t}{A\varepsilon_0\varepsilon_f} = \frac{1}{A\varepsilon_0}\left(\frac{d_{i,Pt/P60}}{\varepsilon_{i,Pt/P60}} + \frac{d_{P60}}{\varepsilon_{P60}} + \frac{d_{i,P60/Pt}}{\varepsilon_{i,P60/Pt}}\right) \quad (1)$$

where, ε_0 (=8.854 × 10^{-12} F m^{-1}) and ε_f are the vacuum permittivity and relative dielectric constants, respectively, ε_i is the relative dielectric constant of interfacial layer between film and electrode and *A* is the capacitor area; d_t, d_{P60} and d_i are the total thickness of the film, thickness of P60 film and thickness of interface layer between Pt and P60 layer, respectively.

As the thickness of the interfacial layer is very small compared to the total thickness, $d_t \gg d_i$, the thickness of the film can be then

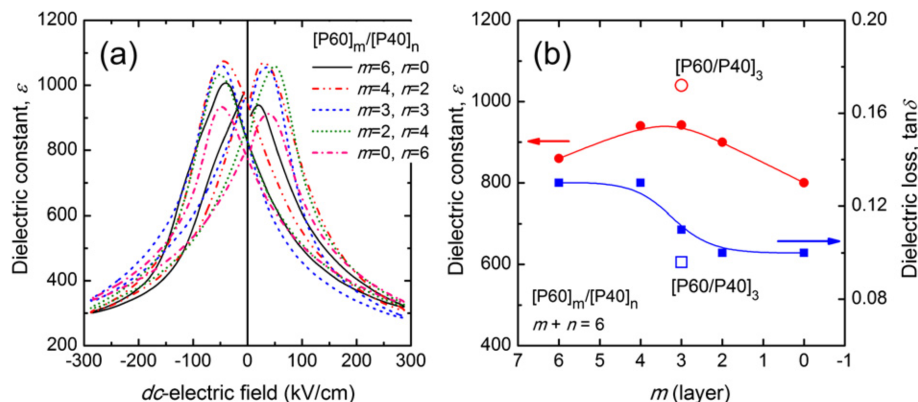

Fig. 7. (a) Dielectric–electric field curves, (b) dielectric constant (ε) and dielectric loss (tan δ) of multilayered $[P60]_6$ and $[P40]_6$, and heterolayered $[P60]_3/[P40]_3$ thin films. The lines are drawn to guide the eyes.

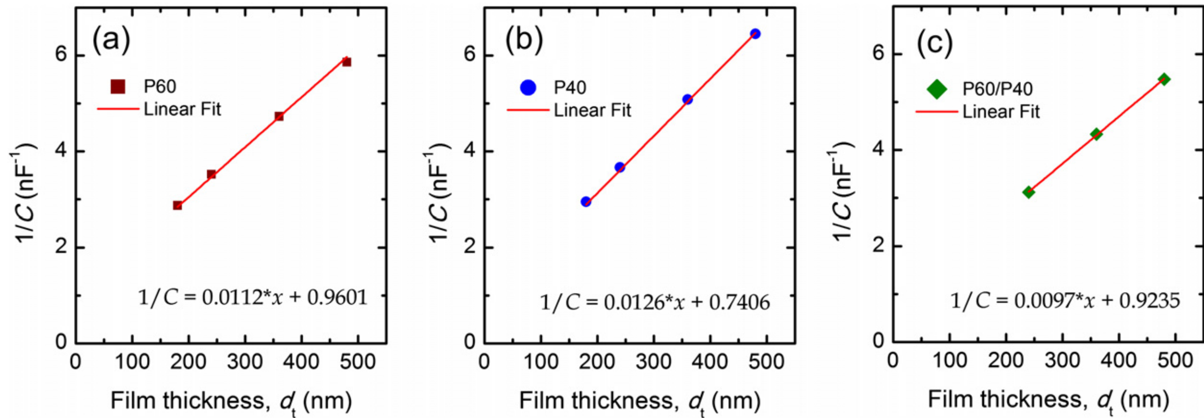

Fig. 8. Inverse capacitance as a function of (a,b) multilayered P60 and P40, and (c) heterolayered P60/P40 film thicknesses.

considered as the total thickness, $d_t = d_{P60}$. Equation (1) is now rewritten as:

$$\frac{1}{C} = \frac{d_t}{A\varepsilon_0\varepsilon_f} = \frac{1}{A\varepsilon_0\varepsilon_{P60}}d_t + \frac{1}{A\varepsilon_0}\left(\frac{d_{i,Pt/P60}}{\varepsilon_{i,Pt/P60}} + \frac{d_{i,P60/Pt}}{\varepsilon_{i,P60/Pt}}\right) \quad (2)$$

From the thickness dependence of the inverse capacitance for multilayered P60 and P40 thin films shown in Fig. 8, the theoretical values of relative dielectric constants are calculated to be about 1008 and 896, respectively, for P60 and P40 films.

To investigate the influence of heterostructure on the dielectric constant of heterolayered thin films, the capacitance series connection (e.g., $[P60]_3/[P40]_3$) has been given in several reports [15,31] as the following equation:

$$\frac{1}{C} = \frac{d_t}{A\varepsilon_0\varepsilon_f} = \frac{1}{A\varepsilon_0}\left(\frac{d_{i,Pt/P60}}{\varepsilon_{i,Pt/P60}} + \frac{d_{P60}}{\varepsilon_{P60}} + \frac{d_{P40}}{\varepsilon_{P40}} + \frac{d_{i,P40/Pt}}{\varepsilon_{i,P40/Pt}}\right) \quad (3)$$

As the thickness of the interfacial layer is very small compared to the total thickness, equation (3) is rewritten as:

$$\frac{1}{C} = \frac{d_t}{A\varepsilon_0\varepsilon_f} = \frac{d_t/2}{A\varepsilon_0\varepsilon_{P60}} + \frac{d_t/2}{A\varepsilon_0\varepsilon_{P40}} + \frac{d_{i,Pt/P60}}{A\varepsilon_0\varepsilon_{i,Pt/P60}} + \frac{d_{i,P40/Pt}}{A\varepsilon_0\varepsilon_{i,P40/Pt}} \quad (4)$$

Assuming that the interfacial layers near the top- and bottom-electrodes of the multilayered PZT thin films are similar, then the values of $d_{i,Pt/P60}/A\varepsilon_0\varepsilon_{i,Pt/P60}$ and $d_{i,P40/Pt}/A\varepsilon_0\varepsilon_{i,P40/Pt}$ can be determined from equation (2) and Fig. 8(a) and (b). The values of $d_{i,Pt/P60}/A\varepsilon_0\varepsilon_{i,Pt/P60}$ and $d_{i,P40/Pt}/A\varepsilon_0\varepsilon_{i,P40/Pt}$ are 0.4800 and 0.3703, respectively, for P60 and P40 multilayered films. The value of relative dielectric constant of heterolayered P60/P40 film can thus be obtained from equation (4), which gives the value of 949. This calculated dielectric constant showed a 22.4% decrease compared to the relative dielectric constant ($\varepsilon_f = 1162$) which is obtained from Fig. 8(c). It suggests that heterolayered thin film cannot be explained as the sum of each individual film (P60 and P40) using a series connection capacitor model [15,17]. In this situation, the influence of interface between the layers with different compositions must be taken into account in the improvement of the dielectric constant in heterolayered $[P60]_3/[P40]_3$ thin film, and therefore equation (3) can now be rewritten with the contribution of P60/P40 interfacial layer:

$$\frac{1}{C} = \frac{d_t}{A\varepsilon_0\varepsilon_f} = \frac{1}{A\varepsilon_0}\left(\frac{d_{i,Pt/P60}}{\varepsilon_{i,Pt/P60}} + \frac{d_{P60}}{\varepsilon_{P60}} + \frac{d_{i,P60/P40}}{\varepsilon_{i,P60/P40}} + \frac{d_{P40}}{\varepsilon_{P40}} + \frac{d_{i,P40/Pt}}{\varepsilon_{i,P40/Pt}}\right)$$
$$= \frac{1}{A\varepsilon_0}\left(\frac{d_{P60}}{\varepsilon_{P60}} + \frac{d_{P40}}{\varepsilon_{P40}}\right) + \frac{d_{i,Pt/P60}}{A\varepsilon_0\varepsilon_{i,Pt/P60}} + \frac{d_{i,P40/Pt}}{A\varepsilon_0\varepsilon_{i,P40/Pt}} + \frac{d_{i,P60/P40}}{A\varepsilon_0\varepsilon_{i,P60/P40}} \quad (5)$$

where $d_{i,P60/P40}$ and $\varepsilon_{i,P60/P40}$ are the thickness and relative dielectric constant of interfacial layer between P60 and P40 layers, respectively. The value of $d_{i,P60/P40}/A\varepsilon_0\varepsilon_{i,P60/P40}$ of 0.0732 is calculated from equation (5) and Fig. 8.

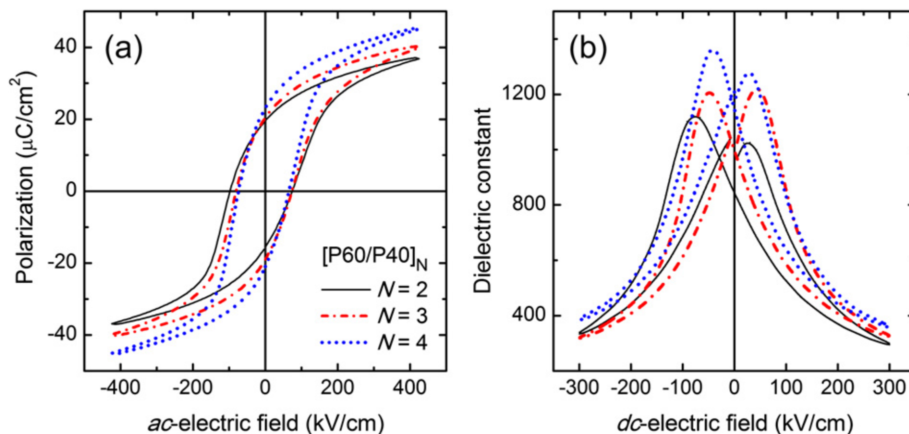

Fig. 9. (a) Polarization hysteresis loops and (b) dielectric constant–electric field curves, of alternating heterolayered $[P60/P40]_N$ thin films with $N = 2$, 3 and 4.

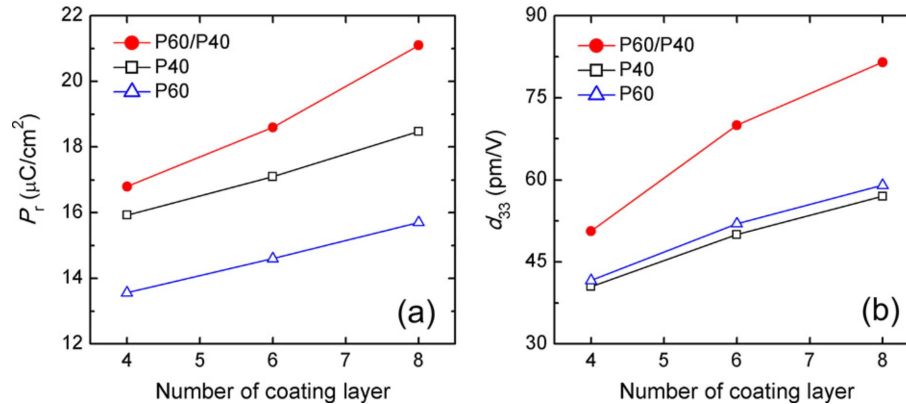

Fig. 10. (a) Remnant polarization (P_r) and (b) effective piezoelectric coefficient ($d_{33,f}$), as a function of the number of coating layers. The lines are drawn to guide the eyes.

The effect of number of coating layers on the ferroelectric and piezoelectric properties in the alternating heterolayered PZT thin films is also studied and shown in Figs. 9 and 10. The values of P_r, ε, and $d_{33,f}$ are found to increase with the number of PZT coating layers. Namely, these parameters are 17.0 μC cm^{-2}, 880 and 48 pm V^{-1}; 18.6 μC cm^{-2}, 1040 and 70 pm V^{-1}; 21.0 μC cm^{-2}, 1190 and 80 pm V^{-1}, for $[P60/P40]_2$, $[P60/P40]_3$, and $[P60/P40]_4$ thin films, respectively. The thickness dependence of P_r in the ferroelectric films might be due to the presence of an interfacial layer that is insulating and/or non-ferroelectric at the film–electrode interface. For very thin films, the presence of an interfacial layer degrades the ferroelectric performance. This layer has less effect on the thicker films, therefore leading to an increase in domain wall mobility, and consequently, an increase in the P_r value as well. The effect of the interfacial layer on the ε value can be explained by pinning centers. In thicker films, a smaller relative volume would be affected by the interfacial pinning centers [32]. This corresponds to an increase in the ε value with increasing film thickness. Moreover, the value of the *dc*-bias field of the two peaks is slightly asymmetric for either the dielectric constant and/or electric field axes, most probably related to the asymmetry between top and bottom interfaces. The thin-film capacitor becomes more symmetrical with increasing coating layer, as shown in Fig. 9(b).

Another important factor affecting the ferroelectric and piezoelectric properties is the mechanical stress that induced from the substrate clamping. Due to mechanical constrains imposed by the substrate, the domain wall motion in PZT thin films is partially clamped and resulted in a decrease in the value of P_r, as well as ε and $d_{33,f}$. On the other hand, the increase in P_r, ε and d_{33} values with increasing film thickness is directly related to the decrease in the residual stress [33]. The influence of the heterolayered structure on the P_r and d_{33} values, moreover, were also investigated from the heterolayered and multilayered films with different film thicknesses. Fig. 10 shows that the P_r and d_{33} values increased with the film thickness in all structures, however, the trend is larger than in the heterolayered film. It is confirmed that there is an influence of the field-induced coupling effect between the tetragonal and rhombohedral phase layers on the properties of heterolayered film in addition to the influence of interfacial layer at the film–electrode interface.

4. Conclusions

Heterolayered and alternating heterolayered PZT thin films deposited onto $Pt/Ti/SiO_2/Si$ wafers have been successfully fabricated by a spin coating assisted sol–gel method. The experimental results showed enhanced ferroelectric and piezoelectric properties in these heterolayered and alternating heterolayered PZT thin films compared to multilayered films. The obtained advantages might be due to the field-induced coupling effect between the rhombohedral and tetragonal phase layers that induces domain switching. The improvement of electrical and mechanical properties for thicker PZT thin films could be explained by the existence of an interfacial layer and substrate clamping. When the film thickness increases, the interfacial layer and substrate clamping have less effect and therefore lead to an increase in domain wall mobility which induces an improvement in domain switching or polarization; as a consequence, the remnant polarization, dielectric constant and piezoelectric coefficient were found to be significantly improved.

Acknowledgments

This work has been supported by the Vietnam's National Foundation for Science and Technology Development (NAFOSTED) under Grant number 103.02-2011.43.

References

[1] J.F. Scott, C.A. Araujo, Science 246 (1989) 1400–1405.
[2] D.L. Polla, L.F. Francis, Annu. Rev. Mater. Sci. 28 (1998) 563–597.
[3] D. Maraldo, K. Rijal, G. Campbell, R. Mutharasan, Anal. Chem. 79 (2007) 2762–2770.
[4] Q. Cui, C. Liu, X.F. Zha, Microfluid. Nanofluid. 3 (2007) 377–390.
[5] T. Alava, F. Mathieu, L. Mazenq, C. Soyer, D. Remiens, L. Nicu, J. Micromech. Microeng. 20 (2010) 075014.
[6] F. Akasheh, T. Myers, J.D. Fraser, S. Bose, A. Bandyopadhyay, Sens. Actuators, A 111 (2004) 275–287.
[7] H.S. Choi, J.L. Ding, A. Bandyopadhyay, M.J. Anderson, S. Bose, J. Micromech. Microeng. 18 (2008) 025037.
[8] J. Baborowski, S. Hediger, P. Muralt, Ch. Wuetrich, Ferroelectrics 244 (1999) 283–290.
[9] D.J. Laser, J.G. Santiago, J. Micromech. Microeng. 14 (2004) R35–R64.
[10] K.S. Yun, E. Yoon, in: T.L. Cornelius (Ed.), MEMS/NEMS Handbook Techniques and Applications, Springer-Verlag, 2006, pp. 121–153.
[11] P. Muralt, IEEE Trans. Ultrason. Ferroelectr. Freq. Control 47 (2000) 903–915.
[12] D.-J. Kim, J.-P. Maria, A.I. Kingon, S.K. Streiffer, J. Appl. Phys. 93 (2003) 5568–5575.
[13] M.D. Nguyen, Ferroelectric and Piezoelectric Properties of Epitaxial PZT Films and Devices on Silicon, PhD Thesis, University of Twente, The Netherlands, 2010.
[14] I. Vrejoiu, Y. Zhu, G.L. Rhun, M.A. Schubert, D. Hesse, M. Alexe, Appl. Phys. Lett. 90 (2007) 072909.
[15] F.C. Kartawidjaja, C.H. Sim, J. Wang, J. Appl. Phys. 102 (2007) 124102.
[16] F. Kartawidjaja, Z. Zhou, J. Wang, J. Electroceram. 16 (2006) 425–430.
[17] F.M. Pontes, E. Longo, E.R. Leite, J.A. Varela, Appl. Phys. Lett. 84 (2004) 5470–5472.
[18] B.A. Tuttle, J.A. Voigt, T.J. Garino, D.C. Goodnow, R.W. Schwartz, D.L. Lamppa, T.J. Headley, M.O. Eatough, in: Proceedings of the Eighth IEEE International Symposium on Applications of Ferroelectrics (ISAF'92), Greenville, USA (September 1992). pp. 344–348.
[19] T. Kumazawa, Y. Kumagai, H. Miura, M. Kitano, K. Kushida, Appl. Phys. Lett. 72 (1998) 608–610.

[20] G.S. Wang, D. Rémiens, E. Dogheche, X.L. Dong, Appl. Phys. A: Mater. Sci. Process. 88 (2007) 657–660.
[21] J. Wang, H. Zheng, Z. Ma, S. Prasertchoung, M. Wuttig, R. Droopad, J. Yu, K. Eisenbeiser, R. Ramesh, Appl. Phys. Lett. 85 (2004) 2574–2576.
[22] S.Y. Yang, F. Zavaliche, L. Mohaddes-Ardabili, V. Vaithyanathan, D.G. Schlom, Y.J. Lee, Y.H. Chu, M.P. Cruz, Q. Zhan, T. Zhao, R. Ramesh, Appl. Phys. Lett. 87 (2005) 102903.
[23] K. Kurihara, M. Kondo, K. Sato, M. Ishii, N. Wakiya, K. Shinozaki, Jpn. J. Appl. Phys. 46 (2007) 6929–6932.
[24] T.A. Berfield, R.J. Ong, D.A. Payne, N.R. Sottos, J. Appl. Phys. 101 (2007) 024102.
[25] Z.H. Zhou, J.M. Xue, W.Z. Li, J. Wang, H. Zhu, J.M. Miao, J. Appl. Phys. 96 (2004) 5706–5711.
[26] L. Lian, N.R. Sottos, J. Appl. Phys. 95 (2004) 629–634.
[27] M.K. Durbin, J.C. Hicks, S.-E. Park, T.R. Shrout, J. Appl. Phys. 87 (2000) 8159–8164.
[28] X.J. Meng, J.L. Sun, J. Yu, L.X. Bo, C.P. Jiang, Q. Sun, S.L. Guo, J.H. Chu, Appl. Phys. Lett. 78 (2001) 2548–2550.
[29] B. Chen, H. Yang, L. Zhao, J. Miao, B. Xu, X.G. Qiu, B.R. Zhao, X.Y. Qi, X.F. Duan, Appl. Phys. Lett. 84 (2004) 583–585.
[30] M. Stengel, N.A. Spaldin, Nature 443 (2006) 679–682.
[31] C. Wang, Q.F. Fang, Z.G. Zhu, A.Q. Jiang, S.Y. Wang, B.L. Cheng, Z.H. Chen, Appl. Phys. Lett. 82 (2003) 2880–2882.
[32] J. Pérez de la Cruz, E. Joanni, P.M. Vilarinho, A.L. Kholkin, J. Appl. Phys. 108 (2010) 114106.
[33] G. Han, J. Ryu, W.-H. Yoon, J.-J. Choi, B.-D. Hahn, D.-S. Park, J. Am. Ceram. Soc. 94 (2011) 1509–1513.